

Automated Identification of Micro-Embolic Events Using Auditory Perception Features Extracted from Mel Frequency Cepstrum Coefficients

Lingke Fan

Department of Medical Physics
University Hospitals of Leicester NHS Trust
Leicester, UK
lingke.fan@uhl-tr.nhs.uk

David H. Evans

Department of Cardiovascular Sciences
University of Leicester
Leicester, UK
dhe@le.ac.uk

Abstract—Directional auditory perception features and energy information were extracted from transcranial Doppler (TCD) ultrasound signals and were used to automatically identify micro-embolic events (MEEs) using a novel embolic signal analysis approach. Three directional analysis methods were evaluated for their MEE identification performance using data recorded during cardiac surgery. The analysis methods were based on Mel frequency cepstrum coefficients (MFCCs), linear frequency cepstrum coefficients (LFCCs) and linear spectral components (LSCs). The results of these preliminary off-line evaluations showed that: a) the auditory perception and energy features of Doppler signals could play an important role in the identification of MEEs; b) MFCC-based analysis seems to be superior to the other two methods, achieving a sensitivity of 95.99%, a specificity of 96.43% and a positive predictive value (PPV) of 95.64%. Future studies using larger data sets and more complicated detection implementation (a rather basic rule-based system was used in the detection stage here) could further confirm or improve the identification performance and robustness of MFCC-based systems.

Keywords—Doppler ultrasound; automated embolus identification; TCD; MFCC application; directional analysis, auditory perceptual evaluation; artifact rejection, knowledge-based systems.

I. INTRODUCTION

Identification of cerebral micro-embolic events (MEEs) utilizing transcranial Doppler (TCD) ultrasound is often used to provide valuable information in clinical and research settings [1]-[3]. Therefore considerable effort has been made using a wide range of signal analysis approaches (e.g., [4]-[7]), trying to improve the reliability of automated MEE identification (AMEEI) systems.

A novel AMEEI approach is proposed in this study with the following objectives:

1. To emulate and use human auditory perceptual features in AMEEI. Human auditory perception plays an important role in manual MEE detection procedures that are often regarded as quite reliable in research settings [8], [9]. Hence perceptual features are studied here to explore their potential to improve AMEEI performance.
2. To extract the directional signatures of embolic signals and apply them in the classification of MEEs. It is widely acknowledged that, in general, MEEs are

unidirectional events whilst artifacts are bi-directional ones [10], [11]. However, the way to efficiently use this directional information for AMEEI purposes is yet to be addressed in detail and in depth.

Three AMEEI methods were evaluated in this study. Mel frequency cepstrum coefficients (MFCCs), linear frequency cepstrum coefficients (LFCCs) and linear spectral components (LSCs) were used to extract basic perceptual and perception-related energy features from recorded signals. Doppler signals containing both sporadic MEEs and embolic showers recorded from patients during cardiac surgery were used to evaluate these methods. A “gold standard” based on the results from manual MEE detection was applied to all the evaluations of the AMEEI performance.

This paper is divided into 5 sections. The details for the design and implementation of the AMEEI methods are given in the next section. Section III contains the details of the clinical data and evaluation procedures. Experimental results, AMEEI performance comparisons and discussion are provided in Section IV, which is followed by conclusions and future work in Section V.

II. METHODS

A. The MFCC-based Directional Analysis Approach

Imagining that a trained human operator is listening to both the forward and reverse Doppler signals to compare the auditory perceptions, the perceived difference between the two signals can be emulated by calculating the directional perceptual distance (DPD) between the two Doppler signals. The DPD at time index n is defined as (the sampling frequency is 12.5kHz and the data window length is 10.24ms):

$$DPD_n = \sqrt{\sum_{i=1}^N [MfccF(i) - MfccR(i)]^2} \Big|_{t=n} \quad (1)$$

Here $MfccF(i)$ and $MfccR(i)$ are the i th MFCC elements (from the “classical” MFCC calculation [12]) for the forward and reverse signals at time index n , respectively; and $N=7$ is the number of the MFCC elements used in the DPD calculation. Based on the DPD, the mean directional perceptual distance (MDPD) and the differential directional

perceptual distance (DDPD) at time index n can be calculated as:

$$\text{MDPD}_n = \frac{1}{100} \sum_{i=n-50}^{n+49} \text{DPD}_n \quad (2)$$

$$\text{DDPD}_n = \text{DPD}_n - \text{MPD}_n \quad (3)$$

An energy parameter is defined in this study as the estimated signal to background ratio (ESBR):

$$\text{ESBR}_i = 10 \log_{10} (\text{EngS}_i / \text{EngB}_i) \quad (4)$$

EngS_i is the estimated signal energy at time index i and EngB_i is the estimated energy (averaged in a 154-ms window) for the background signals around time index i . These energy estimations are calculated using the spectral magnitude elements obtained using a 128-point FFT and a Hamming window (overlap=50%).

Using above results and an 8 frame (40.96ms) moving window, the relative perceptual and energy correlation (RPEC) at time index n can be defined as:

$$\text{RPEC}_n = \frac{8 \sum_{i=n-4}^{n+3} \text{DDPD}_i \text{ESBR}_{F_i} - \sum_{i=n-4}^{n+3} \text{DDPD}_i \sum_{i=n-4}^{n+3} \text{ESBR}_{F_i}}{\sqrt{8 \sum_{i=n-4}^{n+3} \text{DDPD}_i^2 - \left[\sum_{i=n-4}^{n+3} \text{DDPD}_i \right]^2} \sqrt{8 \sum_{i=n-4}^{n+3} \text{ESBR}_{F_i}^2 - \left[\sum_{i=n-4}^{n+3} \text{ESBR}_{F_i} \right]^2}} \quad (5)$$

where ESBR_{F_i} is the ESBR for the forward signal at time index i . The RPEC_n is actually the correlation coefficient between the differential perceptual change and the relative energy variation for the forward signal within the moving window. It should become high for MEEs (the higher the relative embolic signal level in the forward direction, the larger the relative directional perceptual difference) and low for normal artifacts due to their bi-directional properties.

Another directional parameter derived from the RPEC is the averaged relative perceptual and energy correlation (ARPEC) within a positive ESBR_F peak between the two time indexes $n1$ and $n2$ that form the two boundaries of the peak. The ARPEC corresponding to the ESBR_F peak is defined as:

$$\text{ARPEC} = \begin{cases} \frac{1}{J2 - J1 + 1} \sum_{i=J1}^{J2} \text{RPEC}_i, & \text{ESBR}_{F_i} > 0 \text{ for } i = J1, J1+1, \dots, J2; \\ 0, & \text{else} \end{cases} \quad (6)$$

An MFCC-based automated identification unit was designed and developed to detect MEEs with a certain signal threshold (i.e., $\text{ESBR} \geq 7\text{dB}$), using the above defined parameters. Fig.1 shows the block-diagram of this rather basic rule-based system and Table I lists the parameters used and their details.

B. The LFCC-based Directional Analysis Approach

An LFCC-based MEE detection unit was designed and developed using a system structure similar to that shown in Fig.1. The main difference, however, is that the MFCCs and all the MFCC-based parameters were replaced by their LFCC counterparts in the directional/perceptual evaluations. The calculation of the LFCCs is same as that of the MFCCs, except that mel scale filters are not used [12].

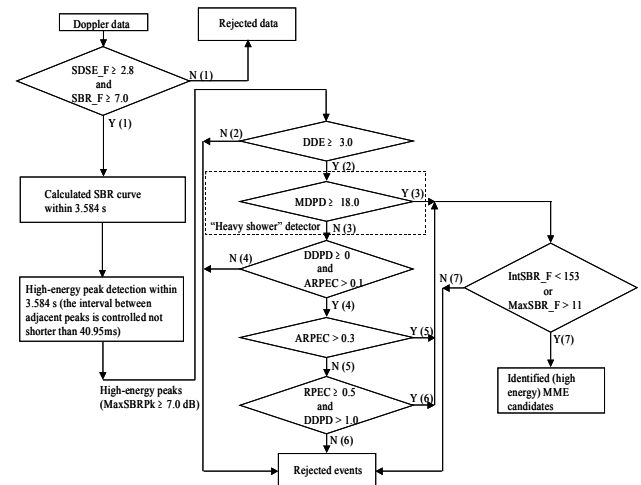


Figure 1. An MFCC-based MEE detection unit. The details of all the parameter are listed in Table I and all the evaluation thresholds were empirically chosen.

TABLE I. THE PARAMETERS USED IN THE MFCC-BASED MEE DETECTION UNIT

Parameter	Details	Units
SDSE_F	The standard deviation of the energy for the forward signal within a 102 ms window.	dB
ESBR_F	The estimated signal to background ratio for the forward signal.	dB
MaxSBRPk	The maximum magnitude within a single positive ESBR_F peak.	dB
DDE	The directional differential energy: the energy of the forward signal minus the energy of the reverse signal.	dB
MDPD	The mean directional perceptual distance within a 512 ms window—see (2).	N/A
DDPD	The differential directional perceptual distance—see (3).	N/A
RPEC	The relative perceptual and energy correlation—see (4).	N/A
ARPEC	The averaged relative perceptual and energy correlation—see (5).	N/A
IntSBR_F	The interval for the longest ESBR_F segment containing all-positive points (within a 3.6 s window). The interval could contain multiple positive ESBR_F peaks.	ms
MaxSBR_F	The maximum ESBR_F value within the IntSBR_F.	dB

The directional linear frequency distance (DLFD) is used as the LFCC counterpart of the (MFCC-based) DPD. The DLFD at the time index n can be defined as:

$$DLFD_n = \sqrt{\sum_{i=1}^N [LfccF(i) - LfccR(i)]^2} \Big|_{t=n} \quad (7)$$

where $LfccF(i)$ and $LfccR(i)$ are the i th LFCC elements for the forward and reverse signals at time index n , respectively; and $N=7$ is the number of the LFCC elements used.

Similar to the calculations in (2), (3), (5) and (6), four more LFCC-based parameters were derived from the DLFD, as the LFCC counterparts of MDPD, DDPD, RPEC and ARPEC. These five LFCC-based parameters were then used to form an LFCC-based MEE detection unit according to the same rule-based system structure shown in Fig.1.

C. The LSC-based Directional Analysis Approach

Again, the same system structure shown in Fig.1 was used to design an LSC-based MEE detection unit. This time, the MFCCs and all the MFCC-based parameters were replaced by their LSC counterparts in the directional/perceptual evaluations.

The directional spectral distance (DSD) is used here to replace the MFCC-based DPD in (1). The DSD at the time index n can be defined as:

$$DSD_n = \sqrt{\sum_{i=1}^{N1} [|XF(i)| - |XR(i)|]^2} \Big|_{t=n} \quad (8)$$

where $|XF(i)|$ and $|XR(i)|$ are the spectral magnitudes for the forward and reverse signals sampled at the i th frequency index, and $N1=46$ was chosen to match the corresponding frequency bandwidth used in the MFCC and LFCC methods.

Using formulae similar to (2), (3), (5) and (6), four more LSC-based parameters are deduced from the DSD, as the analogues of MDPD, DDPD, RPEC and ARPEC. These five LSC-based parameters were then used in an LSC-based MEE detection unit with the same rule-based system structure shown in Fig.1.

III. CLINICAL DATA AND EVALUATION PROCEDURES

A. Data Acquisition

The data used in this study were selected from Doppler recordings on two patients during cardiac surgery (a mitral valve replacement and an aortic root replacement). These recordings were made using a modified version of the in-house multi-gate TCD system previously developed [5]. Doppler signals from only one chosen gate were used in this study. A transmitted frequency of 2 MHz and a pulse repetition frequency of 12.5 kHz were chosen during the signal acquisitions. The receive gate width was set to 10 mm and the sample depth was adjusted to give the optimal signal from the middle cerebral arteries of the patients.

B. MEE Verification Methods

The evaluation started with the identification of significant events (SEs). Here, a SE was defined as an event with the ESR higher than or equal to 7dB. A 40-ms time-

domain resolution was used to find the numbers of SEs in data recordings. A “gold standard” based on the manual “case study decision method” [8] was then used to verify MEEs that were part of the SE family.

C. Data and Procedures for the Training Phase

Four recordings containing 998 seconds of recorded signals in total were used to train the knowledge-based system shown in Fig.1. About 12350 SEs were found in these training data, which included 1756 verified MEEs.

The training data were purposely selected from clinical recordings, to contain sporadic MEEs, MEE groups and artifacts including those caused by diathermy signals.

The training data were used for setting and tuning the thresholds and parameters in all the three analysis methods (i.e., the MFCC-based, the LFCC-based and the LSC-based approaches), until the “optimized” training performances were reached for these three AMEEI systems.

D. Data and Evaluation Procedures for the Testing Phase

The system was evaluated in two ways using data different from those recordings used in the training phase.

First, an evaluation of sporadic MEE identification was performed using three recordings, which had a total signal duration of 827 seconds. These recordings contained 2,835 SEs, 128 sporadic MEEs and many artifacts including those caused by diathermy signals.

Second, an evaluation of the ability to detect closely packed MEEs was carried out, using one recording that was dominated by heavy embolic showers. The recording contained 4,547 SEs within the recording duration of 310 seconds, amongst which 3,189 were verified as MEEs (closely packed MEEs were separated using 7-dB ESR peaks during the verification).

The results of the two evaluations were then used to obtain the overall evaluation results for all three AMEEI methods being tested.

IV. EVALUATION RESULTS AND DISCUSSION

A. Evaluation Results for Sporadic MEE Identification

The sensitivity, the specificity and the positive predictive value (PPV) results for the evaluation of sporadic MEE identification are shown in Table II. It can be seen that the MFCC-based AMEEI method outperforms the other two methods in all the categories, although the performances of the other two methods are also reasonably good.

An example of identification of sporadic MEEs using the MFCC-based method is shown in Fig.2 (the display results for the LFCC-based and the LSC-based methods are not provided since they are identical to Fig.2 in this example).

B. Evaluation Results for the Identification of MEEs in Heavy Embolic Showers

The results for this evaluation are shown in Table III. The performance for the MFCC-based method demonstrates an excellent sensitivity, a moderate PPV and a slightly lower specificity. The number of non-embolic events is relatively

low in this 5 minute recording containing heavy embolic showers, compared with the number of MEEs.

As an example for comparison, Fig.3, Fig.4 and Fig.5 show the MFCC-based, the LFCC-based and the LSC-based

methods used to detect a group of MEEs within an embolic shower, and yellow indicator lines are used to mark identified MEEs.

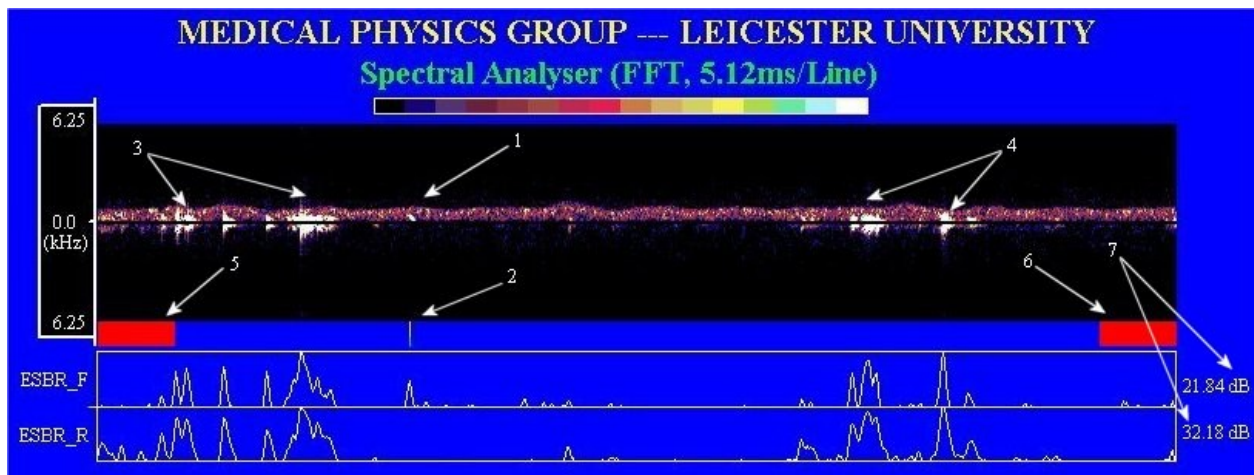


Figure 2. An example of detecting sporadic MEEs using the MFCC-based method. The sonograms for the forward and reverse Doppler signals are displayed on the upper part of the screen, whilst the estimated signal to background ratios (ESBRs) are shown on the lower part of the screen (ESBR_F is for the forward signal and ESRB_R is for the reverse). Arrow 1 shows a sporadic MEE. Arrow 2 demonstrates that the MEE has been detected by the MFCC-based method, with a yellow indicator displayed under the sonogram. Arrows 3 and 4 point to artefacts. Arrows 5 and 6 indicate non-detection regions of the sonograms for the current screen (i.e., any MEE within these regions is to be identified in the previous or subsequent screen). Arrow 7 points to the display range for the ESRB_F and ESRB_R.

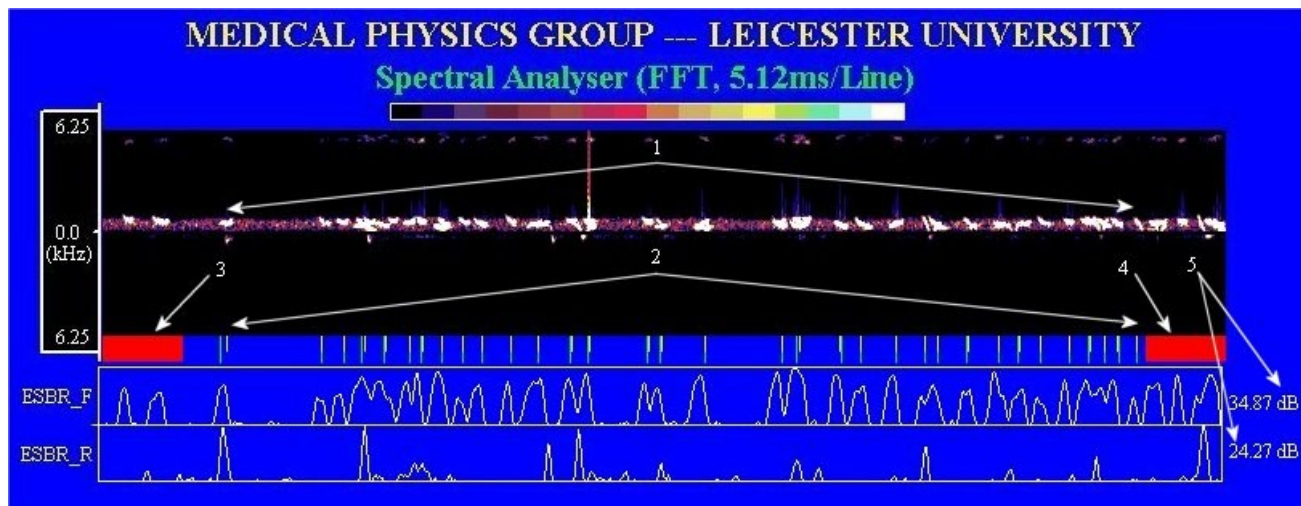


Figure 3. An example of detecting MEEs in the heavy embolic showers using the MFCC-based method. The sonograms for the forward and reverse Doppler signals are displayed on the upper part of the screen, whilst the estimated signal to background ratios (ESBRs) are shown on the lower part of the screen (ESBR_F is for the forward signal and ESRB_R is for the reverse). Arrow 1 shows a group of MEEs within an embolic shower. Arrow 2 demonstrates that the MEEs have been verified using the manual "gold standard" (green lines displayed under the sonogram) and also detected by the MFCC-based method (with yellow indicator lines displayed). It can be seen that the automated method detects the EBSR_F peaks more accurately, compared to the manual verifications. Arrows 3 and 4 indicate non-detection regions of the sonograms for the current screen (i.e., any MEE within these regions is to be identified in the previous or subsequent screen). Arrow 5 points to the display range for the EBSR_F and EBSR_R.

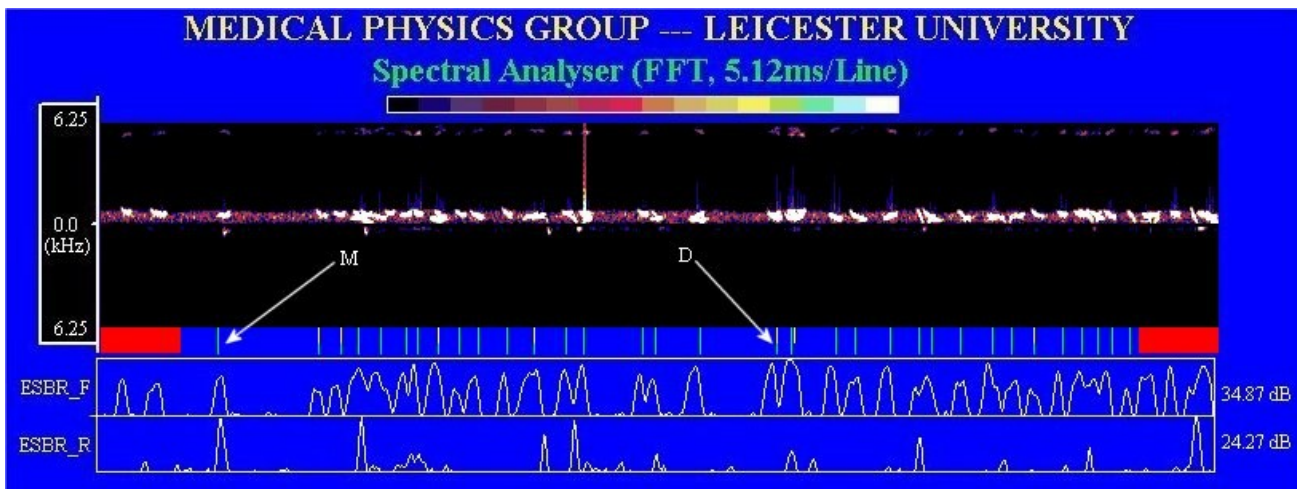


Figure 4. An example of detecting MEEs in the heavy embolic showers using the LFCC-based method. The sonogram and ESBR displays are the same as those in Fig.3, except for the following differences: (a) a green indicator shows that a MEE is verified by the manual “gold standard” but missed by the LFCC-based method (as shown in an example indicated by Arrow “M”); (b) a green indicator overlapped by a yellow one demonstrates that a MEE is manually verified and also automatically detected by the LFCC-based method (as shown in an example indicated by Arrow “D”).

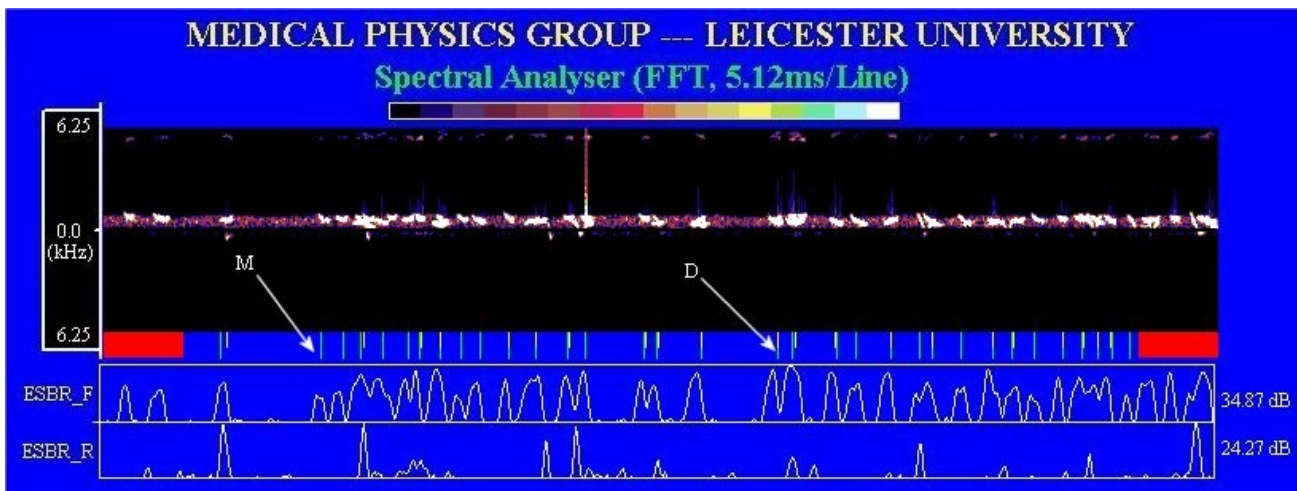


Figure 5. An example of detecting MEEs in the heavy embolic showers using the LSC-based method. The sonogram and ESBR displays are the same as those in Fig.3, except for the following differences: (a) a green indicator shows that a MEE is verified by the manual “gold standard” but missed by the LSC-based method (as shown in an example indicated by Arrow “M”); (b) a green indicator overlapped by a yellow one demonstrates that an MEE is manually verified and also automatically detected by the LSC-based method (as shown in an example indicated by Arrow “D”).

C. Overall Evaluation Result

The overall evaluation results for the automated MEE identification are shown in Table IV. It shows that, with similar specificity and PPV results for all the three methods, the MFCC-based AMEEI system seems to be significantly superior in terms of sensitivity performance.

TABLE II. EVALUATION RESULTS FOR SPORADIC MEE IDENTIFICATION

AMEEI Method	Automated Identification Performances (Data duration: 827s, 2835 SEs & 128 MEEs)		
	Sensitivity	Specificity	PPV
MFCC-based	97.67%	99.93%	98.43%
LFCC-based	88.28%	99.89%	97.41%
LSC-based	96.09%	99.08%	83.11%

TABLE III. EVALUATION RESULTS FOR THE IDENTIFICATION OF MEEs IN HEAVY EMBOLIC SHOWERS

AMEEI Method	Automated Identification Performances (Data duration: 310s, 4547 SEs & 3189 MEEs)		
	Sensitivity	Specificity	PPV
MFCC-based	95.92%	89.47%	95.53%
LFCC-based	38.29%	95.58%	95.32%
LSC-based	64.85%	95.14%	96.91%

TABLE IV. OVERALL EVALUATION RESULTS

AMEEI Method	Automated Identification Performances (Data duration: 1137s, 7382 SEs & 3317 MEEs)		
	Sensitivity	Specificity	PPV
MFCC-based	95.99%	96.43%	95.64%
LFCC-based	40.22%	98.45%	95.49%
LSC-based	66.05%	97.76%	96.01%

D. Discussion

It seems from the results that all the three methods performed reasonably well while detecting sporadic MEEs. It should be noticed that the MFCC-based method is superior to other two methods, with a higher sensitivity as well as a higher specificity.

Furthermore, the MFCC-based method coped quite well with heavy embolic showers, whilst the other two methods suffered heavy sensitivity losses. Our in-depth investigations revealed that the LFCC and the LSC parameters were not sensitive enough to follow the rapid directional signal changes due to heavy embolic showers, which could be the cause for the significant numbers of MEEs missed by these two detection approaches.

The results also demonstrated that even the simpler conventional spectral based LSC method outperformed the LFCC-based approach in general.

V. CONCLUSIONS AND FUTURE WORK

A novel MFCC-based embolic signal analysis has been proposed to explore the potentials of auditory perception and energy features of Doppler signals in automated embolus identification. Initial off-line evaluations were carried out using Doppler signals recorded during cardiac surgery and the results show the proposed method could play an important role in a high-performance automated MEE identification system. Compared with the LFCC-based and the traditional LSC-based approaches, the MFCC-based method seems to have a superior performance in both cases of sporadic MEEs and with heavy embolic showers.

Further clinical evaluations with a larger data set will be necessary in future studies.

All the approaches at this stage were applied based on an assumption that an artery had already been located by an

operator (i.e., sonograms had been established and displayed). Future studies could be carried out to include the searching phase while the operator is locating the artery. Since unidirectional artifacts could be occasionally generated (e.g., due to a finger touching on the probe) in this rather special detection phase, additional signal analysis measures may be needed to cope with these unwanted events.

ACKNOWLEDGMENT

The authors sincerely thank Emma Chung and Rachel Summer for their help collecting the clinical data during cardiac surgery.

REFERENCES

- [1] E.V. Van Zuilen, J. Van Gijn and R.G.A. Ackerstaff, "The clinical relevance of cerebral microemboli detection by transcranial Doppler ultrasound," *J. Neuroimaging*, vol. 8, pp. 32-37, Jan. 1998.
- [2] D.H. Evans, "Detection of microemboli," in *Transcranial Doppler ultrasonography*, VL Babikian and LR Wechsler, Eds. Boston: Butterworth Heinemann, 1999, pp. 141-155.
- [3] R. Dittrich and E.B. Ringelstein, "Occurrence and clinical impact of microembolic signals during or after cardiosurgical procedures," *Stroke*, vol. 39, pp. 503-511, Feb. 2008.
- [4] H. Markus, M. Cullinane and G. Reid, "Improved automated detection of embolic signals using a novel frequency filtering approach," *Stroke*, vol. 30, pp. 1610-1615, August 1999.
- [5] L. Fan, E. Boni, P. Tortoli and D.H. Evans, "Multigate transcranial Doppler ultrasound system with real-time embolic signal identification and archival," *IEEE Trans Ultrason Ferroelectr Freq Control*. Vol. 53, pp. 1853-1861, Oct. 2006.
- [6] D. Kouamé, M. Biard, J.M. Girault and A. Bleuzen, "Adaptive AR and neurofuzzy approaches: access to cerebral particle signatures," *IEEE Trans Inf Technol Biomed.*, vol. 10, pp. 559-566, July 2006.
- [7] H.S. Ng, Q. Hao, T. Leung, K.S. Lawrence Wong, H. Nygaard, J.M. Hasenkam and P. Johansen, "Embolus Doppler ultrasound signal detection using continuous wavelet transform to detect multiple vascular emboli," *J Neuroimaging*, vol. 18, pp. 388-95, Oct. 2008.
- [8] L. Fan, D.H. Evans and A.R. Naylor, "Automated embolus identification using a rule-based expert system," *Ultrasound Med Biol*. Vol. 27, pp. 1065-1077, August 2001.
- [9] Dittrich R, M.A. Ritter, M. Kaps, M. Siebler, K. Lees, V. Larrue, D.G. Nabavi, E.B. Ringelstein, H.S. Markus and D.W. Droste, "The use of embolic signal detection in multicenter trials to evaluate antiplatelet efficacy: signal analysis and quality control mechanisms in the CARESS (Clopidogrel and Aspirin for Reduction of Emboli in Symptomatic carotid Stenosis) trial," *Stroke*, vol. 37, pp. 1065-1069, April 2006.
- [10] EB Ringelstein, DW Droste, VL Babikian, DH Evans, DG Grosset, M Kaps, HS Markus, D Russell and M Siebler, "Consensus on microembolus detection by TCD. International Consensus Group on Microembolus Detection," *Stroke*, vol. 29, pp. 725-729, March 1998.
- [11] M Saqqur, N Dean, M Schebel, MD Hill, A Salam, A Shuaib and AM Demchuk, "Improved detection of microbubble signals using power M-mode Doppler," *Stroke*, vol. 35, pp. e14-17, Jan. 2004.
- [12] S.B. Davis and P. Mermelstein, "Comparison of parametric representations for monosyllabic word recognition in continuously spoken sentences," *IEEE Trans Acoustics, Speech and Signal Processing*. Vol. ASSP-28, pp. 357-366, August 1980.